Clinical Radiology 74 (2019) 818.e1–818.e7

Contents lists available at ScienceDirect

Clinical Radiology

journal homepage: www.clinicalradiologyonline.net

Machine learning-based texture analysis for differentiation of large adrenal cortical tumours on CT

M.M. Elmohr [a], D. Fuentes [a], M.A. Habra [b], P.R. Bhosale [c], A.A. Qayyum [c], E. Gates [a], A.I. Morshid [a], J.D. Hazle [a], K.M. Elsayes [c,*]

[a] Department of Imaging Physics, The University of Texas MD Anderson Cancer Center, Houston, TX, USA
[b] Department of Endocrine Neoplasia and Hormonal Disorders, The University of Texas MD Anderson Cancer Center, Houston, TX, USA
[c] Department of Diagnostic Radiology, The University of Texas MD Anderson Cancer Center, Houston, TX, USA

ARTICLE INFORMATION

Article history:
Received 31 January 2019
Accepted 27 June 2019

AIM: To compare the efficacy of computed tomography (CT) texture analysis and conventional evaluation by radiologists for differentiation between large adrenal adenomas and carcinomas.

MATERIALS AND METHODS: Quantitative CT texture analysis was used to evaluate 54 histopathologically proven adrenal masses (mean size=5.9 cm; range=4.1–10 cm) from 54 patients referred to Anderson Cancer Center from January 2002 through April 2014. The patient group included 32 women (mean age at mass evaluation=59 years) and 22 men (mean age at mass evaluation=61 years). Adrenal lesions seen on precontrast and venous-phase CT images were labelled by three different readers, and the labels were used to generate intensity- and geometry-based textural features. The textural features and the attenuation values were considered as input values for a random forest-based classifier. Similarly, the adrenal lesions were classified by two different radiologists based on morphological criteria. Prediction accuracy and interobserver agreement were compared.

RESULTS: The textural predictive model achieved a mean accuracy of 82%, whereas the mean accuracy for the radiologists was 68.5% ($p<0.0001$). The interobserver agreements between the predictive model and radiologists 1 and 2 were 0.44 ($p<0.0005$; 95% confidence interval [CI]: 0.25–0.62) and 0.47 ($p<0.0005$; 95% CI: 0.28–0.66), respectively. The Dice similarity coefficient between the readers' image labels was 0.875±0.04.

CONCLUSION: CT texture analysis of large adrenal adenomas and carcinomas is likely to improve CT evaluation of adrenal cortical tumours.

Introduction

The discovery of incidental adrenal masses on imaging has become progressively more frequent as the number of radiological scans obtained for different diagnostic

* Guarantor and correspondent: K. M. Elsayes, Department of Diagnostic Radiology, The University of Texas MD Anderson Cancer Center, 1400 Pressler Street, Houston, TX, 77030, USA. Tel.: +713-745-3025; Fax: +713-794-4379.
E-mail address: kmelsayes@mdanderson.org (K.M. Elsayes).

https://doi.org/10.1016/j.crad.2019.06.021
0009-9260/

purposes has increased. The prevalence of incidental adrenal masses on computed tomography (CT) imaging is estimated to be as high as 4.2%.[1] On further evaluation, the majority of these masses turn out to be benign; around 75% are adrenocortical adenomas (ACAs),[2,3] whereas around 2% are adrenocortical carcinomas (ACCs),[4] being rare primary adrenal tumours that account for only 0.02% of all malignancies.[5,6] Several clinical and radiological features, including a tumour size <4 cm and a pre-contrast attenuation <10 HU, suggest that a mass is benign, while a tumour size >4 cm, necrosis, haemorrhage, and/or a high precontrast attenuation >10 HU — particularly >43 HU — may suggest malignancy.[7–12] Meanwhile, indeterminate lesions, measuring 4 cm with or without any of the previous radiological features, present a diagnostic challenge and are mostly resected for pathological identification[13]; however, although 25–30% of resected lesions exceed 4 cm at diagnosis, most are not malignant (Fig 1). An adrenal CT protocol, comprised of a precontrast phase, a venous phase (60–80 seconds after injection of intravenous contrast material), and a delayed phase (15 minutes after contrast medium injection), represents the mainstay of the classification of adrenal lesions and has a specificity approaching 100% for lipid-rich adenomas.[14]

Radiomics involves the analysis of diagnostic images and its transformation into quantifiable features that provide richer information that will potentially increase the value of imaging and assist in clinical decision-making.[15] Several studies have explored the utilisation of CT texture analysis, a biomarker for assessment, and evaluation of mass heterogeneity on CT, to predict tumour histology, grade, and response to treatment. Texture analysis has been performed on many organs, including brain, lungs, liver, stomach, and pancreas,[16–19] and it was recently used in conjunction with manual tumour segmentation of kidney lesions to accurately differentiate renal cell carcinoma from fat-poor angiomyolipoma.[20]

The purpose of this retrospective study was to compare the diagnostic potentials of CT texture analyses of large adrenal adenomas and carcinomas >4 cm and conventional radiological assessments by human readers.

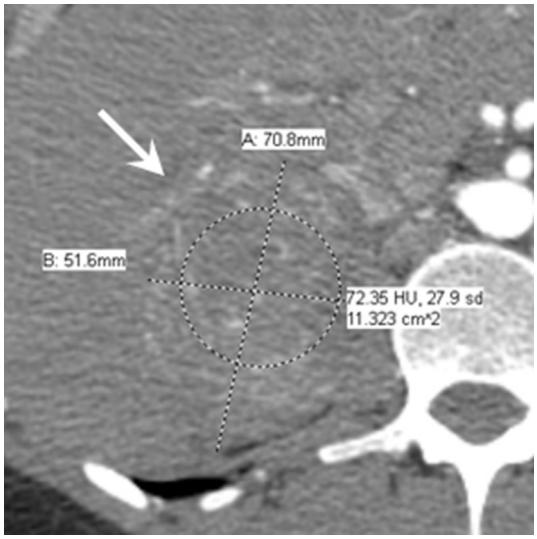

Figure 1 Contrast-enhanced axial CT image of a 30-year-old woman with a right adrenocortical adenoma. Preoperative CT demonstrated a 7.1×5.2 cm well-circumscribed mass (arrow) within the right adrenal gland; the attenuation value was 72 HU, suggestive of malignancy. The adrenal mass was surgically resected and proven at histopathological examination to be adrenocortical adenoma. It was categorised as malignant by both blinded readers; however, the CT texture analysis model was able to correctly categorise the lesion as benign.

Materials and methods

Patient population

This retrospective study was approved by the institutional review board and informed consent requirement was waived. The patients, who were selected from a database of patients with large adrenal lesions (>4 cm) and who had been included in a previously published paper assessing interobserver agreement in the characterisation of large adrenal tumours >4 cm,[21] were referred to MD Anderson Cancer Center from January 2002 through April 2014. All patients had undergone surgical resection of the lesions, and the resected specimens had been histopathologically examined. In total, 54 patients were identified, including 32 women (mean age at mass evaluation=59 years; range=30–78 years) and 22 men (mean age at mass evaluation=61 years; range=31–83 years). The mean age at diagnosis was 52 years. Of the 54 patients, 29 had ACC and 25 had ACA. Data on hormonal status, symptoms related to the adrenal mass, past medical history, and social history were obtained from the patients' electronic medical records. The patients' demographic and tumour characteristics are summarised in Table 1.

Table 1
Patient demographics and tumour characteristics.

Characteristic	Value (n=54)
Mean age at diagnosis	
ACA	53 years (range, 27–67 years)
ACC	51 years (range, 31–78 years)
Sex	M=22, F=32
Tumour type	
ACA	25
ACC	29
Mean tumour size, cm	
ACA	5.9 (range, 4.1–10)
ACC	8.4 (range, 4.4–17)
Tumour side	
Right	21
Left	29
Bilateral	4
Clinical symptoms	
Hormonal hypersecretion	24 (44%)
Compressive symptoms	22 (41%)
Family history of malignancy	39 (72%)
Personal history of malignancy	10 (19%)
Alive at last follow-up	34 (63%)

ACA, adrenocortical adenoma; ACC, adrenocortical carcinoma; F, female; M, male.

CT imaging data

Preoperative abdominal CT was obtained using an adrenal protocol comprised of a precontrast phase, a venous phase (60–80 seconds after injection of intravenous contrast material), and a delayed phase (15 minutes after contrast injection). Scans were performed on 64 multidetector CT Light-Speed scanners (GE Healthcare, Waukesha, WI, USA) with a pitch of 1–1.5, a rotation time of 0.5–0.8 seconds, a section thickness of 2.5 mm, and a standard reconstruction algorithm. The injection rate was 3–5 ml/s. Delayed phase CT images were included for calculation of contrast medium washout percentages.

Abdominal CT images had previously been independently reviewed by two different board-certified radiologists (P.B., with >10 years of experience in abdominal imaging, and A.Q., with >15 years of experience in abdominal imaging). The two radiologists were not involved in the initial read of these cases in clinical setting and were blinded to the final results of the histopathological examinations of the resected masses.[21] For comparison purposes, the morphological characteristics of the patients' tumours (precontrast attenuation, number of calcifications, shape, percentage of fat, heterogeneity, degree of necrosis, washout percentages, and tumour margin) were evaluated based on a three-point scale (1=probably benign, 2=indeterminate, and 3=probably malignant). For each tumour, a subjective radiological impression of benign, indeterminate, or malignant was reported on the basis of these factors and the radiologist's overall impression. Several of the previous characteristics were found to significantly correlate with the tumours' nature (benign versus malignant); lesions with round shape, visible fat, low precontrast attenuation, and a subjective radiological impression of benignity were significantly more likely to represent ACAs ($p<0.05$). The majority of lesions that were rated indeterminate by each reader were found to be malignant (71%). The number of calcifications, heterogeneity, margin, and the degree of necrosis were not correlated with the histopathological diagnosis.

Data curation and texture analysis

The precontrast and venous phase CT studies (obtained 60–80 seconds after contrast medium administration) were exported in DICOM format from the picture archiving and communication system to an independent server. Subsequently, the images were converted into the format recommended by the Neuroimaging Informatics Technology Initiative, compressed, and reoriented into right-anterior–inferior orientation by the Convert3D image-processing tool.[22]

The lesions were manually segmented by three different readers for assessment of inter-reader variability in the segmented margins. Segmentation was performed using Amira Software (Thermo Scientific, Waltham, MA, USA; Fig 2).[23] The lesion masks and the greyscale CT images were imported into the PyRadiomics platform version 2.1.1[24] for image texture analysis. First-order statistics, shape-based features, and the image features for the grey-level co-occurrence matrix, the grey-level run length matrix, the grey-level size zone matrix, the neighboring grey-tone difference matrix, and the grey-level dependent matrices were extracted for each lesion.[24,25] Definitions of each radiomic feature were based on the definitions provided in [26].

Statistical analysis

Modelling and analysis were implemented using the statistical computing software R version 3.2.5 (The R Foundation for Statistical Computing, Vienna, Austria).[27] Inter-reader variability in regard to the evaluation of the labelled lesions was assessed using the variance of the Dice similarity coefficient (DSC). In regard to the radiological

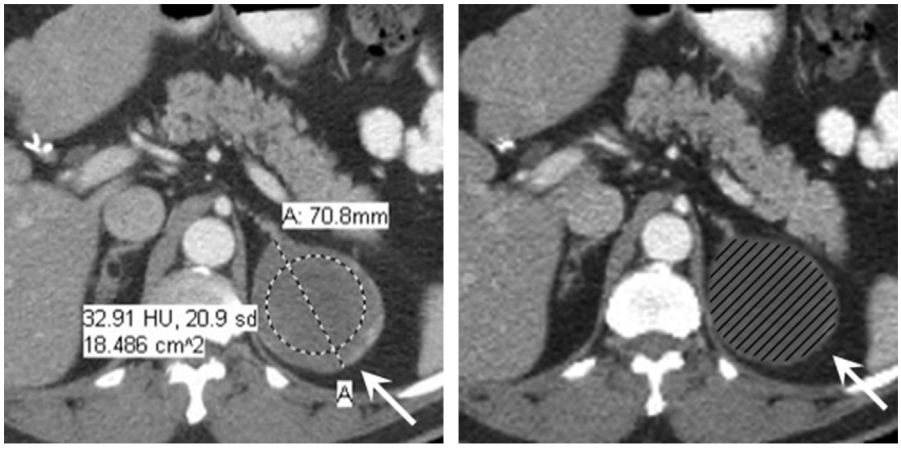

Figure 2 Contrast-enhanced axial CT image of a 60-year-old man with an incidental left adrenocortical adenoma. Preoperative CT (a) demonstrated a well-circumscribed mass (arrow) measuring 7.1×6.3 cm within the left adrenal gland; the attenuation value was 33 HU on the venous phase. The left adrenal gland (arrow) was manually segmented in (b). The mass was correctly classified as benign by both human readers and the CT texture analysis model.

impressions of the adrenal masses, interobserver agreement between the CT texture analysis model and each reader was measured using Cohen's kappa coefficient (k).

Because a large number of image features were generated during the analysis, variable reduction was performed to identify highly predictive variables and reduce redundant information.[28] To accomplish this, correlation reduction was applied to the input variable (with a cut-off of 0.8); logistic regression and the Boruta feature selection algorithm were then used to assess important features for predicting lesion class.[28] Boruta is a feature selection algorithm based on random forest that iteratively excludes variables that are shown to have predictive performance comparable to random fluctuations.[29] Textural variables and radiological features were expressed as medians with ranges. Differences between the two tumour classes (ACCs versus ACAs) in regard to the image features and radiological variables were ascertained using Wilcoxon's signed rank test; a p-value of <0.05 was considered statistically significant. Two prediction models were constructed: one that used the image features, and one that used the image features in combination with the tumour attenuation values determined on CT (Fig 3). Prediction accuracy was evaluated using a leave-one-out training–testing paradigm.

Results

The adrenal lesions were right sided in 21 patients, left sided in 29 patients, and bilateral in four patients. Ten patients (19%) had a personal history of non-adrenal malignancies, and 34 (63%) were alive at last follow-up.

Interobserver agreement was calculated between the CT texture analysis model and each reader. Moderate agreement was observed between the predictive model and reader 1 (k=0.44; $p<0.0005$; 95% CI: 0.25–0.62) and between the predictive model and reader 2 (k=0.47; $p<0.0005$; 95% CI: 0.28–0.66). The diagnostic accuracy was 61% for reader 1 and 76% for reader 2 (mean accuracy=68.5%).

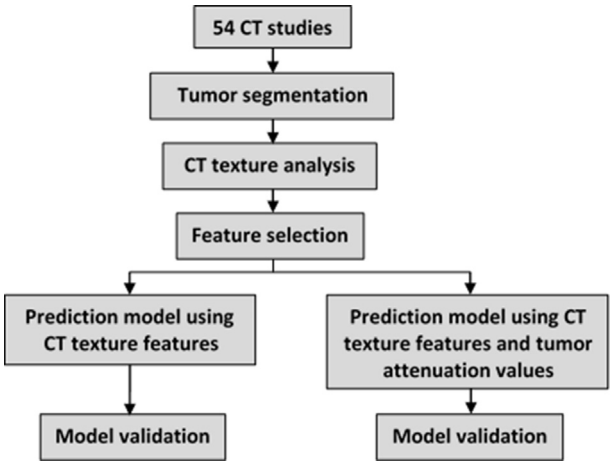

Figure 3 Flowchart summarising the CT texture analysis and classification process.

To evaluate the reliability of the segmentations, the DSC (0.875±0.04) was used to perform comparisons between the repeated segmented volumes. After variable reduction, 18 CT textural features were found to be statistically significant and correlated with tumour class (variables are summarised in Table 2, and box and whisker plots are shown in Fig 4). Of the radiological features, the CT attenuation value in the unenhanced studies showed a positive correlation with the tumour class; ACA masses had median attenuation of 19.5 HU, and ACC masses had a median attenuation of 34 HU ($p=0.006$). Conversely, the attenuation difference (attenuation difference=venous phase attenuation − precontrast phase attenuation) showed a negative correlation; ACA masses had median attenuation difference of 59.5 HU, while ACC masses had median attenuation difference of 20 HU ($p=0.004$). Several textural features had statistical significance; for example, some grey-level-based features, such as the GLSZM high grey level emphasis, were positively correlated with malignancy in ACC masses, which had larger values averaging around 5.3×10^7 compared to an average of 3.3×10^6 in ACAs; higher values denote more heterogeneity of the tumour mass.

The reduced CT texture features and the attenuation values were used as the input values for a Boruta random forest algorithm for the binary classification of masses as ACC or ACA. Table 3 provides a summary of the prediction accuracy observed for the univariate logistic regression and the Boruta random forest models. A leave-one-out classification accuracy of 82% ($p<0.00001$; 95% CI: 0.69–0.92) was achieved for differentiation of the lesions using the univariate logistic regression model (which used CT texture features combined with attenuation values); the receiver operating characteristic curve is shown in Fig 5; however, when the CT texture features without attenuation values were used to differentiate between lesions, the univariate logistic regression and Boruta random forest methods attained a classification accuracy of 61% and 76%, respectively.

Discussion

The present findings from the precontrast and venous phase CT texture analysis of adrenal adenomas and carcinomas >4 cm suggest that CT texture analysis, in combination with CT attenuation values, is likely to improve radiological evaluation by human readers.

In the present study, the relatively subjective radiological evaluations by the readers blinded to the histopathological examination results were compared with the more objective CT texture analyses. In a previous study, the interobserver agreement between human readers regarding the overall assessment of tumours as benign or malignant was low (k=0.26), underscoring the subjectivity and inconsistency of conventional adrenal tumour.[21] In contrast, the present predictive model utilising CT texture analysis combined with CT attenuation values achieved a significantly higher diagnostic accuracy (82%) than did the radiologists (68.5%) in classifying adrenal tumours >4 cm as

Table 2
Results of computed tomography (CT) texture and attenuation value analysis.

Variable	ACA			ACC			*p*-Value
	Minimum	Maximum	Median	Minimum	Maximum	Median	
Precontrast phase features							
GLSZM zone percentage	0.02	0.1	0.05	0.01	0.07	0.03	<0.005
GLRLM run variance	0.27	5.3	0.66	0.4	4.1	1.7	<0.005
GLSZM high grey-level emphasis	1.2×10^{6}	1.1×10^{9}	3.3×10^{6}	8.1×10^{5}	2.5×10^{10}	5.3×10^{7}	<0.005
Shape-based maximum 2D diameter section	40.3	194.2	50.8	28	123.8	79.2	0.005
Attenuation value	-17	51	19.5	17	82	34	<0.05
Venous phase features							
First order total energy	2.5×10^{7}	1.3×10^{9}	2.4×10^{8}	2.7×10^{7}	4×10^{10}	6.8×10^{8}	<0.005
GLSZM grey-level non-uniformity	51.6	4393	194.8	58.2	1800	556	<0.005
Attenuation difference[a]	1	111	59.5	-3	69	20	<0.05

A *p*-value of <0.05 was considered statistically significant.
ACA, adrenocortical adenoma; ACC, adrenocortical carcinoma; GLRLM, grey-level run length matrix; GLSZM, grey-level size zone matrix. GLRLM, grey-level run length matrix.
[a] Attenuation difference, attenuation on venous phase − attenuation on precontrast phase.

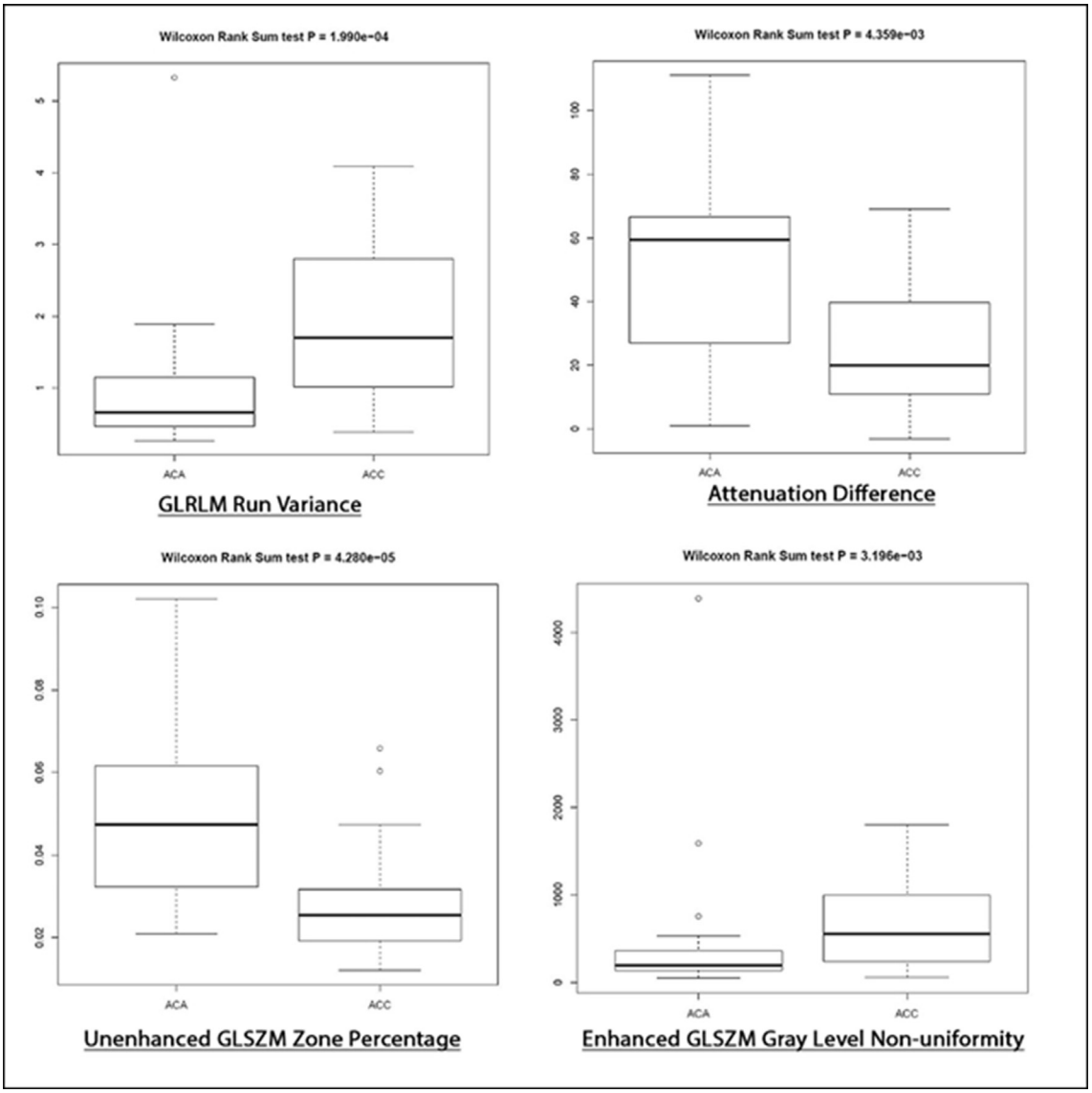

Figure 4 Box and whisker plots for several CT textural features and attenuation. *A *p*-value of <0.05 was considered statistically significant.

Table 3
Prediction models of statistical significance.

Model	Accuracy	95% CI	NIR	p-value[a]	Sens	Spec	NPV	PPV	AUC
Univariate logistic regression (CT texture features + attenuation values)	0.82	0.69–0.92	0.53	0.00001	0.81	0.83	0.8	0.85	0.89
Boruta random forest (CT texture features)	0.76	0.62–0.87	0.54	0.0006	0.76	0.76	0.73	0.79	0.83

AUC, area under the receiver operating characteristic curve; CI, confidence interval; NIR, no information rate; NPV, negative predictive value; PPV, positive predictive value; sens, sensitivity; spec, specificity.
[a] A p value < 0.05 was considered statistically significant.

benign or malignant. Furthermore, CT texture analysis yielded significantly consistent results during testing and retesting, as demonstrated by the high DSC (0.875±0.04).

The present results demonstrated a positive correlation between the heterogeneity of a lesion and the risk of malignancy. A multitude of features on CT texture analysis verified increased attenuation (measured by grey level) and heterogeneity in ACCs compared to ACAs, which have a more uniform texture. ACCs have been known to exhibit heterogeneous enhancement on contrast CT images owing to the presence of haemorrhage, calcification, and central necrosis commonly seen in malignant adrenal lesions; in contrast, adenomas show relatively homogeneous enhancement.[30] In the present study, ACCs were associated with a higher attenuation value (median=34 HU; p=0.006) compared to ACAs (median=19.5 HU; p=0.006). These results agree with previous findings that textural features correlate with the underlying pathology.[31]

Similar observations have been documented by Romeo *et al.*,[32] who showed that employing magnetic resonance imaging (MRI) textural features, specifically the 3D maximum diameter, led to superior diagnostic performance in the characterisation of adrenal lesions on unenhanced MRI compared with a senior radiologist.

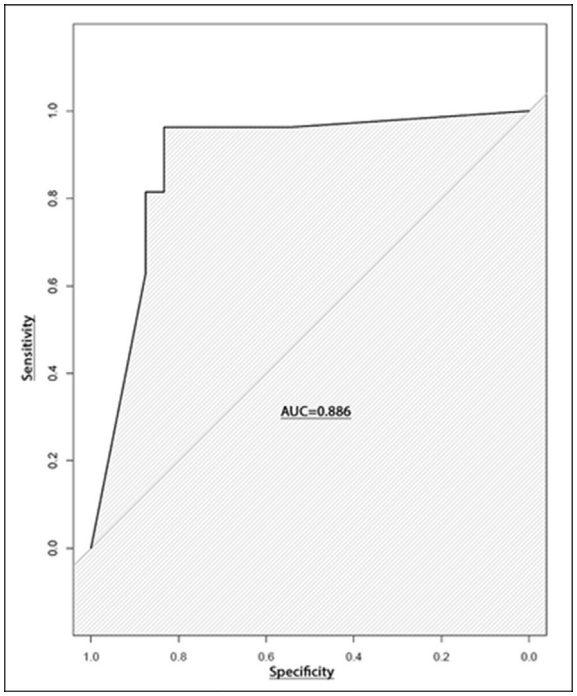

Figure 5 Receiver operating characteristic curve for univariate logistic regression for CT textural features combined with attenuation values.

There are several limitations in this study. First, the present retrospective study was performed using a small sample size (n=54), as well as nearly equivalent proportions of adrenal adenomas and carcinomas, which is unreflective of the actual prevalence of these tumours. To assess the reproducibility of the results, a more realistic ACC percentage and a larger patient population are required. Second, the study is limited by the highly selective nature of the included tumours, i.e., ACAs, and ACCs. The inclusion of adrenal metastases and adrenal phaeochromocytomas would have been optimal, given the fact that their diagnosis can be challenging on imaging. Third, delayed-phase CT images were not included in the present study because the CT studies of 26 patients (48%) had inconsistent post-contrast delay times (e.g., 5-minute delays instead of 15-minute delays). The inclusion of the delayed images could possibly have increased the diagnostic accuracy of the CT texture analysis model.[10,27–29] Finally, although, the achieved prediction accuracy of 82% seems satisfyingly high, it also means that one out of five large adrenal lesions would be classified incorrectly. To address these limitations, further study of a larger population with typical adrenal CT protocol images would be optimal and might achieve higher prediction accuracy.

In conclusion, CT texture analysis, in combination with CT attenuation values and attenuation differences, could improve conventional evaluations by human readers for the accurate classification of large adrenal lesions into adenomas and carcinomas and could potentially assist radiologists and other physicians in diagnostic evaluations. The present study achieved consistent prediction accuracies. Further studies on larger patient populations are warranted.

Conflicts of interest

The authors declare no conflict of interest.

References

1. Davenport C, Liew A, Doherty B, *et al*. The prevalence of adrenal incidentaloma in routine clinical practice. *Endocrine* 2011;**40**(1):80–3.
2. Barzon L, Sonino N, Fallo F, *et al*. Prevalence and natural history of adrenal incidentalomas. *Eur J Endocrinol* 2003;**149**(4):273–85.
3. Song JH, Chaudhry FS, Mayo-Smith WW. The incidental adrenal mass on CT: prevalence of adrenal disease in 1,049 consecutive adrenal masses in patients with no known malignancy. *AJR Am J Roentgenol* 2008;**190**(5):1163–8.

4. Cawood TJ, Hunt PJ, O'Shea D, *et al*. Recommended evaluation of adrenal incidentalomas is costly, has high false-positive rates and confers a risk of fatal cancer that is similar to the risk of the adrenal lesion becoming malignant; time for a rethink? *Eur J Endocrinol* 2009;**161**(4):513.
5. Young Jr WF. Management approaches to adrenal incidentalomas. A view from Rochester, Minnesota. *Endocrinol Metab Clin N Am* 2000;**29**(1):159–85.
6. Lipsett MB, Hertz R, Ross GT. Clinical and pathophysiologic aspects of adrenocortical carcinoma. *Am J Med* 1963;**35**(3):374–83.
7. Ng L, Libertino JM. Adrenocortical carcinoma: diagnosis, evaluation and treatment. *J Urol* 2003;**169**(1):5–11.
8. Barzon L, Scaroni C, Sonino N, *et al*. Incidentally discovered adrenal tumours: endocrine and scintigraphic correlates. *J Clin Endocrinol Metab* 1998;**83**(1):55–62.
9. Singh PK, Buch HN. Adrenal incidentaloma: evaluation and management. *J Clin Pathol* 2008;**61**(11):1168–73.
10. Caoili EM, Korobkin M, Francis IR, *et al*. Adrenal masses: characterization with combined unenhanced and delayed enhanced CT. *Radiology* 2002;**222**(3):629–33.
11. Bharwani N, Rockall AG, Sahdev A, *et al*. Adrenocortical carcinoma: the range of appearances on CT and MRI. *AJR Am J Roentgenol* 2011;**196**(6):W706–14.
12. Blake MA, Kalra MK, Sweeney AT, *et al*. Distinguishing benign from malignant adrenal masses: multi-detector row CT protocol with 10-minute delay. *Radiology* 2006;**238**(2):578–85.
13. Zeiger MA, Thompson GB, Duh QY, *et al*. The American association of clinical endocrinologists and American association of endocrine surgeons medical guidelines for the management of adrenal incidentalomas. *Endocr Pract* 2009;**15**(Suppl. 1):1–20.
14. Boland GW, Lee MJ, Gazelle GS, *et al*. Characterization of adrenal masses using unenhanced CT: an analysis of the CT literature. *AJR Am J Roentgenol* 1998;**171**(1):201–4.
15. Avanzo M, Stancanello J, El Naqa I. Beyond imaging: the promise of radiomics. *Phys Med* 2017;**38**:122–39.
16. Ganeshan B, Goh V, Mandeville HC, *et al*. Non-small cell lung cancer: histopathologic correlates for texture parameters at CT. *Radiology* 2013;**266**:326.
17. Ganeshan B, Burnand K, Young R, *et al*. Dynamic contrast-enhanced texture analysis of the liver: initial assessment in colorectal cancer. *Invest Radiol* 2011;**46**:160.
18. Eilaghi A, Baig S, Zhang Y, *et al*. CT texture features are associated with overall survival in pancreatic ductal adenocarcinoma — a quantitative analysis. *BMC Med Imaging* 2017;**17**(1):38.
19. Nanthagopal AP, Rajamony RS. A region-based segmentation of tumour from brain CT images using nonlinear support vector machine classifier. *J Med Eng Technol* 2012;**36**(5):271–7.
20. Hodgdon T, McInnes MD, Schieda N, *et al*. Can quantitative CT texture analysis be used to differentiate fat-poor renal angiomyolipoma from renal cell carcinoma on unenhanced CT images? *Radiology* 2015;**276**:787.
21. Thomas AJ, Habra MA, Bhosale PR, *et al*. Interobserver agreement in distinguishing large adrenal adenomas and adrenocortical carcinomas on computed tomography. *Abdom Radiol* 2018;**43**(11):3101–8.
22. Yushkevich PA, Piven J, Hazlett HC, *et al*. User-guided 3D active contour segmentation of anatomical structures: significantly improved efficiency and reliability. *NeuroImage* 2006;**31**(3):1116–28.
23. ThermoFischer Scientific. Amira for life & biomedical sciences. Available at: https://www.thermofisher.com/uk/en/home/industrial/electron-microscopy/electron-microscopy-instruments-workflow-solutions/3d-visualization-analysis-software/amira-life-sciences-biomedical.html. June 23rd, 2018.
24. van Griethuysen JJM, Fedorov A, Parmar C, *et al*. Computational radiomics system to decode the radiographic phenotype. *Cancer Res* 2017;**77**(21):e104–7.
25. Haralick RM, Shanmugam K, Dinstein I. Textural features for image classification. *IEEE Trans Syst Man Cybernet* 1973;**SMC-3**(6):610–21.
26. Hatt M, Vallieres M, Visvikis D, *et al*. IBSI: an international community radiomics standardization initiative. *J Nucl Med* 2018;**59**(Suppl. 1). 287-287.
27. RStudio. RStudio. Available at: https://www.rstudio.com/products/rstudio/. June 23rd, 2018.
28. Sanchez-Pinto LN, Venable LR, Fahrenbach J, *et al*. Comparison of variable selection methods for clinical predictive modeling. *Int J Med Inform* 2018;**116**:10–7.
29. Kursa MB, Rudnicki WR. Feature selection with the Boruta package. *J Stat Softw* 2010;**36**(11):1–13.
30. Singh KSHR. A comparison of grey-level run length matrix and grey-level co-occurrence matrix towards cereal grain classification. *Int J Comp Eng Technol (IJCET)* 2016;**7**(6):9–17.
31. Ng F, Ganeshan B, Kozarski R, *et al*. Assessment of primary colorectal cancer heterogeneity by using whole-tumour texture analysis: contrast-enhanced CT texture as a biomarker of 5-year survival. *Radiology* 2013;**266**(1):177–84.
32. Romeo V, Maurea S, Cuocolo R, *et al*. Characterization of adrenal lesions on unenhanced MRI using texture analysis: a machine-learning approach. *J Magn Reson Imaging* 2018 Jul;**48**(1):198–204.